Experimental and numerical study of the laminar flow in helically coiled pipes

Jacopo De Amicis [1], Antonio Cammi[*], Luigi P.M. Colombo, Marco Colombo [2], Marco E. Ricotti

Department of Energy, Politecnico di Milano, Via Lambruschini 4, 20156 Milano, Italy

Article history:
Received 16 April 2013
Received in revised form
6 May 2014
Accepted 17 May 2014
Available online 14 June 2014

1. Introduction

In the field of research on innovative Nuclear Power Plants (NPPs), the main goals for the future of the nuclear industry have been identified by the Generation IV International Forum (GIF). In particular, the four macro-areas of sustainability, economy, safety & reliability and resistance to proliferation represent the most critical points for the future exploitation of the nuclear source for the power production (GIF, 2010). In order to reach such objectives many different designs are currently being studied and some radical innovations are going to be implemented in the development of the new Generation IV (Gen IV) projects. Together with the Gen IV projects, for the short/medium term other typologies of plant are in the design stage, e.g. the Small-medium Modular Reactors (SMRs), which present some advantages especially from the economical and safety points of view, as they adopt an integral layout, where all the primary system components are located inside the reactor vessel (IAEA, 2005). In this sense, of crucial importance becomes the design of the Steam Generator (SG). Some of these designs are characterized by the adoption of the helical tubes for the SGs, i.e. IRIS (Carelli et al., 2004), NuScale and SMART (Kim et al., 2003) modular reactors. Helical tube SGs are interesting as they provide a larger heat exchange surface with limited volumes within the plant, therefore allowing a global reduction of realization costs (Bejan and Kraus, 2003). Helical tubes are commonly used for several applications beyond the nuclear industry: refrigeration and heating, chemical and process plants, food industry among many others.

However, helical geometry causes a number of distinctive phenomena in the flow field, which differs greatly from that of a more common straight pipe. The curvature of the duct imposes a centripetal force on the fluid, which is forced in a curved trajectory by the channel walls: a certain pressure gradient is produced within the section of the pipe, with a higher value toward the external bend of the duct. A recirculation motion is promoted inside the channel cross section, giving rise to two counter-rotating vortices

* Corresponding author. Tel.: +39 02 2399 6332; fax: +39 02 2399 8566.
E-mail addresses: antonio.cammi@polimi.it, antonio.cammi@gmail.com (A. Cammi).
[1] Present address: EDF Energy R&D UK Centre, University of Manchester, Manchester, United Kingdom.
[2] Present address: Institute of Particle Science and Engineering, School of Process, Material and Environmental Engineering, University of Leeds, Leeds LS2 9JT, United Kingdom.

that are symmetrical in the case of a toroidal pipe. In addition, the axial symmetry typical of the velocity field of a straight channel is broken and the maximum of axial velocity is displaced toward the external direction of the tube. From the engineering point of view, the most important effects are a general increase of the pressure drop along the pipe and of the convective heat transfer coefficients, caused by the intense recirculation and mixing of the fluid within the coiled duct.

This work is focused on the study of single-phase, incompressible laminar flow through helically coiled pipes. At first, the problem is faced from an experimental point of view, by presenting the results obtained in a test facility built at SIET laboratories, in Piacenza, Italy, which reproduces the SG of the IRIS reactor. Pressure drop measured as a function of the mass flow rate is compared with the prediction of different correlations available in literature, in order to evaluate their predictive capability in the considered range of Reynolds numbers. The transition from laminar to turbulent flow is also analyzed, confronting the results with empirical correlations reported in literature. Moreover, the phenomenon is studied through different numerical codes in order to obtain an approximated solution of the hydraulic problem. The various effects linked to the complex geometry of the duct are addressed, by computing and visualizing different relevant quantities, as the axial velocity and the pressure field within the cross sectional area, which are difficult to analyze without the adoption of such computational instruments. Numerical values of the friction factor at different values of Reynolds number are compared with the experimental data obtained at SIET laboratories to evaluate the capability of the different considered codes to reproduce the experimental measurements. In addition, some literature experimental data obtained in other geometrical configurations are also considered in the comparison, together with the correlations previously considered.

2. The flow in helically coiled ducts

Different studies on the fluid flow in helical coils were made in the past, in order to understand the effect of geometry on the quantities of physical and engineering relevance (Berger et al., 1983; Ali, 2001; Naphon and Wongwises, 2006).

Dean (1927, 1928) analyzed toroidal pipes with an analytical approach, developing expressions for the effects induced by geometry on axial velocity and pressure fields. Introducing the hypothesis of small curvature, he obtained a set of equations that describe the velocity field within the tube cross section as that of a straight duct with a centrifugal force. He derived also a correlation for the friction factor along the tube, introducing a non-dimensional quantity defined as:

$$De = Re\sqrt{(r/R)} \tag{1}$$

where r is the tube radius, while R is the coil radius. The above parameter was later renamed Dean number (De), as it was often chosen as a representative quantity in several correlations concerning curved pipes. Wang (1981) expanded Dean's analysis to curved pipes with non-zero torsion, in order to understand its effects on the flow. He developed a non-orthogonal coordinate system, which required a tensorial analysis to derive the desired conservation equations. According to Wang's results, the effect of the torsion τ on the velocity is of the first order, thus comparable to that of the curvature κ. Germano (1982, 1989), starting from Wang reference system, introduced proper modifications in order to obtain an orthogonal coordinate system, that allowed to write directly the differential operators necessary to the definition of the conservation equations. He thus simplified the problem and, in contrast to Wang, concluded that the effect of τ is of the second order, therefore negligible with respect to κ in the majority of the engineering applications.

As concerns the experimental study of the problem, the first experiments were conducted by Eustice (1910) who firstly noticed a certain decrease in the mass flow rate (at constant Δp) in curved pipes with respect to straight ones with the same diameter. He also noticed a difference in the transition between laminar and turbulent flow with respect to straight tubes: in presence of a non-zero curvature κ, such transition is characterized by a smoother behavior of the friction factor across the critical value of the Reynolds number Re_{crit}. Moreover, such critical value is higher than that in straight pipes and it depends on the radius of the helix R. White (1929) conducted several tests on helical coiled tubes with different values of r/R, in order to verify the validity of Dean's model to predict the effect of curvature on the friction pressure drop. He also confirmed that the phenomenology of the transition to turbulent regime depends on both the radius of the helix and the ratio r/R. Ito (1959, 1969), as a consequence of experimental and analytical studies, proposed the following expression for the friction factor, valid in the laminar flow regime:

$$\frac{f_c}{f_s} = \frac{21.5De}{(1.56 + \log_{10}De)^{5.73}} \tag{2}$$

where f_c and f_s are the friction factors for curved and straight pipes, respectively. He also proposed an expression for the critical Re as a function of the ratio (r/R):

$$Re_{crit} = 2 \times 10^4 (r/R)^{0.32} \tag{3}$$

Yamamoto et al. (1995) investigated in detail the effect of the torsion on the flow. The authors found that for increasing values of the non-dimensional torsion parameter $\beta_0 = \tau_{ad}/(2\kappa_{ad})^{0.5}$, friction factor tends to become similar to those of a straight tube. Cioncolini and Santini (2006) analyzed deeply the effect of curvature and torsion on the onset of turbulence. In particular, they tested twelve different geometries, characterized by different curvature and torsion. Hence, they found quite a complex tendency of the critical Reynolds number Re_{crit} with respect to such parameters, completing the description introduced by White: for mild curvatures, the behavior of f_D was similar to that of straight pipes, with a sudden increase around the critical Reynolds number Re_{crit}. Instead, for very high curvatures, they found a single discontinuity in the derivative of the friction factor, which marked the transition between laminar and turbulent flow. Finally, for medium curvatures, they noticed the presence of a depression in the intermediate zone between the fully developed laminar and turbulent regions. Many other researchers studied the phenomenon and proposed numerous correlations for the friction factor valid in the laminar region, which are reported in Table 1.

Table 1
Different correlations compared with experimental data obtained at SIET laboratories.

Correlation	Validity range	Reference
$f_s/f_c = 1 - [1 - (11.6/De)^{0.45}]^{1/0.45}$	$11.6 < De < 2000$	White (1929)
$f_c/f_s = 0.37(0.5De)^{0.36}$	$40 < De < 2000$	Prandtl (1949)
$f_c/f_s = 0.556 + 0.0969\sqrt{De}$	Laminar flow	Hasson (1955)
$f_c/f_s = 21.5De/(1.56 + \log_{10}De)^{5.73}$	$13.5 < De < 2000$	Ito (1959)
$f_c/f_s = 0.509 + 0.0918\sqrt{De}$	Laminar flow	Barua (1963)
$f_c/f_s = 1080\sqrt{De}/(1 - 3.253\sqrt{De})$	$13.5 < De < 2000$	Mori and Nakayama (1965)
$f_c = 32/Re$	$11.6 < De < 30$	Srinivasan et al. (1968)
$f_c = 5.22(Re\sqrt{r/R})^{-0.6}$	$30 < De < 300$	
$f_c = 1.8(Re\sqrt{r/R})^{-0.5}$	$300 < De < De_{cr}$	

In the latest decades, thanks to the diffusion of more and more powerful computers, several authors have faced the problem by means of numerical methods. McConalogue and Srivastava (1968) treated Dean's equations through an expansion in Fourier series and calculated the relative coefficients with an iterative scheme. They showed that for high values of *De* the maximum value of the axial velocity was shifted toward the outer bend of the tube. This causes the viscous stresses (and thus the loss in flow rate or, at constant flow rate, the head losses) to increase, since they are proportional to the velocity gradient, which is higher near the external side of the wall. Greenspan (1973) analyzed the problem of the toroidal duct in order to extend the validity of the previous studies. In particular, he noted the distortion of the streamlines of the secondary flow with increasing *De*, together with the displacement of the maximum of axial velocity u_{max} from the center of the tube section. Murata et al. (1981) studied the problem of the helical coil both from an analytical and a numerical point of view. They described the geometry through the parameter β, which is the angle between the tangential direction of the helix and the horizontal plane (if a helix with vertical rotation axis is considered). The parameter β influences the symmetry of the secondary flow, producing a distortion that causes the displacement of the maximum axial velocity from the normal direction. Hüttl et al. (1999) developed a finite volume method to study Germano's problem, with particular attention to the effect of torsion on the flow characteristics. They used a system of equations analogous to those presented in Germano (1982) and analyzed the effect of τ and *Re* at fixed curvature.

3. The experimental analysis

The experimental facility, built and operated at SIET laboratories, is an extension of an electrically heated test section used to study the thermal hydraulics inside a helical coiled SG tube (Santini et al., 2008). Coil geometry is representative of SG pipe dimensions of a typical SMRs of integral design; coil diameter is 1 m, with a pipe inner diameter of 12.53 mm; full scale facility is 8 m in height and tube length is 32 m. The main parameters of the facility are reported in Table 2.

The conceptual sketch of the new facility is depicted in Fig. 1, whereas a global view of the coil is provided in Fig. 2. In the sketch, two parallel tubes are included, since the same facility was adapted to study also two-phase instability phenomena in parallel tubes, as Density Wave Oscillations (DWOs) and Ledinegg instabilities (Papini et al., 2011, 2014). For the measurement of the pressure drop, only one of the tubes was used, keeping closed the inlet valve of the second one (V2). The whole facility is made by a supply section and a test section. The supply section feeds demineralized water from a tank to the test section through a centrifugal booster pump and a volumetric feed water pump. The flow rate is controlled by a throttling valve (V3) positioned downwards the feed water pump and after a bypass line. System pressure control is accomplished by acting on a throttling valve (V4) placed at the end of the steam generator. An electrically heated preheater is located before the test section, and allows creating the desired temperature at the inlet of the test section. For the current analysis we did not use such preheater, as experiments were conducted with single-phase water flowing at constant ambient temperature.

Table 2
Parameter of the helical coiled tube used at SIET.

Tube material	SS AISI 316L
Inner diameter	12.53 mm
Outer diameter	17.24 mm
Helix diameter	1000 mm
Helix pitch per turn	800 mm
Tube length	32 m
Helix height	8 m
κ_{ad}	0.0118
τ_{ad}	3.00×10^{-3}
λ	0.255

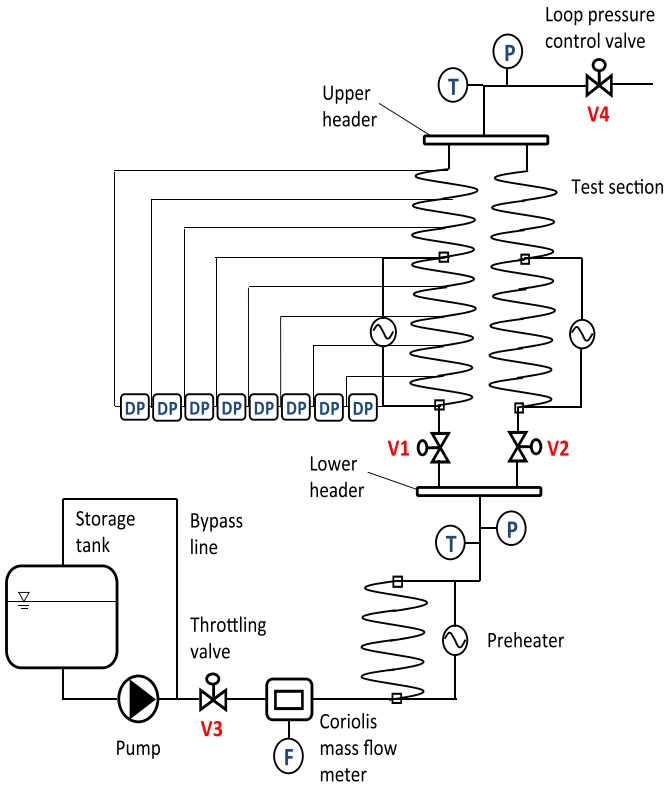

Fig. 1. Scheme of the facility used for the experimentations.

The water pressure at inlet and outlet headers is measured by absolute pressure transducers; nine pressure taps are located nearly every 4 m along the tube and eight differential pressure transducers connected with the taps. An accurate measurement of the flow rate is obtained using a Coriolis flow-meter, placed between the pump and the preheater. Bulk temperatures are measured with K-class thermocouples drowned in a small well at SG inlet and outlet headers. All the measurement devices have been tested and calibrated at the certified SIET laboratories. The following operations were carried out in order to obtain the measurements of the quantities of interest:

1. registration of the elevation head: the tube was filled with water and the relative pressure differences in the manometers were recorded, in order to calculate the gravitational pressure loss;
2. regulation of the system pressure: valve V4 was set in order to obtain the desired pressure at the outlet section of the helical pipe;
3. regulation of the water flow rate: valve V3 was controlled allowing the supply system to give the desired flow rate for the experiment;
4. measurement: when the system reached a stationary state, measures were taken; an appropriate measurement time interval was considered, to obtain a statistically reliable value for the measured parameters;
5. change in flow rate: step 3 was repeated to get the new desired flow rate.

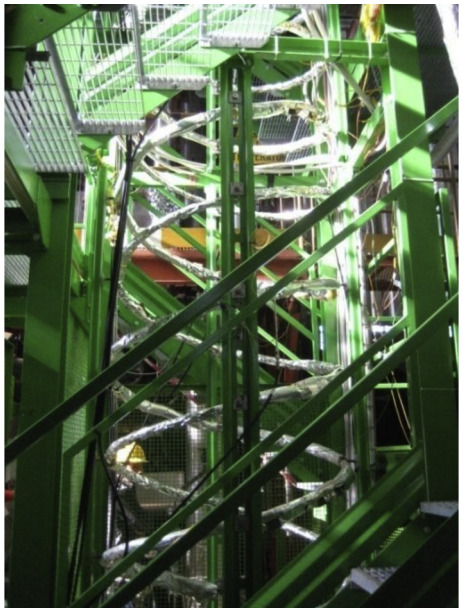

Fig. 2. Picture of the helical coiled pipe installed at SIET laboratories.

Tests were made at an outlet pressure (after valve V4) equal to the ambient one and with water at room temperature at the inlet. The temperature was measured in the lower header and resulted equal to about 20 °C with a maximum deviation of 1.5 °C.

The measured values of differential pressures and flow rates have been analyzed in order to represent the behavior of the friction factor with the Reynolds number. It is important to note that tests were performed in laminar, transition and turbulent regimes, so that we could have a global vision of the behavior of the pressure losses in the helical pipe. The Darcy friction factor f_D was calculated as:

$$f_D = \Delta p \frac{d}{L} \frac{2}{\rho u^2} \tag{4}$$

where Δp is the pressure drop, L is the tube length, d is the internal diameter of the tube and u is the mean velocity across the section.

The behavior of the Darcy friction factor with the Reynolds number is plotted in Fig. 3. The values of f_D were obtained by properly averaging during time the measurements taken by the different independent sensors. Numerous acquisitions were available for every experimental condition, each one including the data from the different pressure transducers. As a consequence, each experimental point is a mean between numerous equivalent measurements, with an error bar representing their standard deviation. A change in slope is clearly visible at a value of *Re* between 3000 and 4000, marking the transition to turbulent flow. Using the formulae provided in Cioncolini and Santini (2006) for medium-curvature coils, the transition point can be estimated as:

$$\frac{R}{r} = 81.0 \rightarrow Re_{crit} = 12,500\left(\frac{R}{r}\right)^{-0.31} \tilde{} 3200 \tag{5}$$

which is in good agreement with the experimental observations. Ito's correlation provided in relation (3) instead gives a less precise prediction of the critical Reynolds number. In Fig. 3 the friction factor is provided: at low flow rates, data for laminar regime lie on a curve which is interrupted with a first discontinuity located at a Reynolds number value defined by relation (5). In the figure,

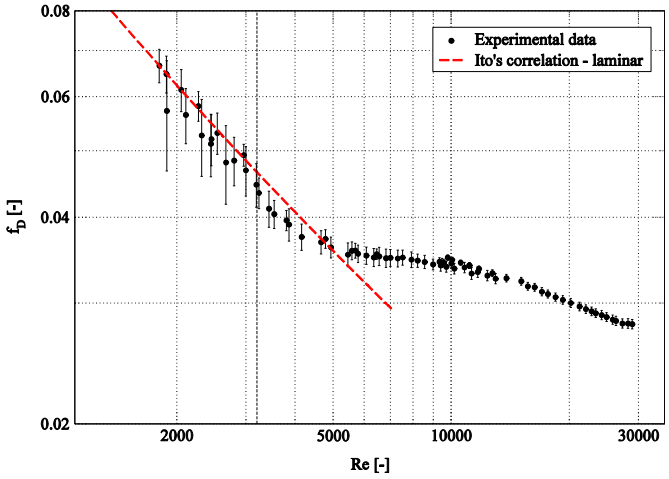

Fig. 3. Behavior of the Darcy friction factor with Reynolds number for the helical coiled pipe installed at SIET laboratories.

deviation from the linear trend of the laminar region attests the discontinuity. To better evidence this change in trend, a typical correlation for the laminar friction factor in helical tubes is plotted together with the data. Moreover, the predicted value of $Re = 3200$ is highlighted. After such discontinuity, a different trend of f_D is found: as predicted in Cioncolini and Santini (2006), a region with lower friction factor is found in the range of *Re* between 3200 and 5000, which is typical of "medium curvature coils". For higher values of the Reynolds number a different curve, characteristic of fully turbulent regime, is found.

In Fig. 4 experimental data in the laminar regime are compared with different correlations presented in literature: as it is shown in the figure all the tested correlations are in satisfactory agreement with the experimental results. However, the effectiveness of the same correlations in the transition region was also analyzed: after *Re* ~3200, almost all the correlations start to lose accuracy in predicting the real value of the friction factor, because of the onset of turbulence. The limiting point of the transition region was chosen at a Reynolds number of approximately 5000, as it corresponds to the location of the second discontinuity which marks the end of the turbulence emerge process and the reaching of fully turbulent flow conditions, marked by a power-law behavior of the friction factor.

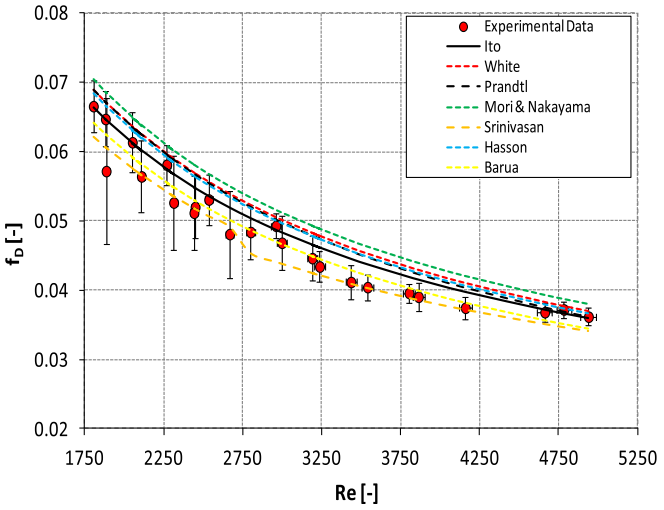

Fig. 4. Comparison between experimental data and different correlations available in literature.

Table 3
Root mean square errors of the correlations compared with experimental data.

Correlation	$Error_{(Re \leq 3200)}$	$Error_{(Re \leq 5000)}$
Ito	4.14%	4.03%
White	3.70%	4.92%
Prandtl	3.57%	4.40%
Mori and Nakayama	4.88%	6.55%
Hasson	3.40%	4.33%
Barua	6.56%	5.77%
Srinivasan	9.53%	8.37%

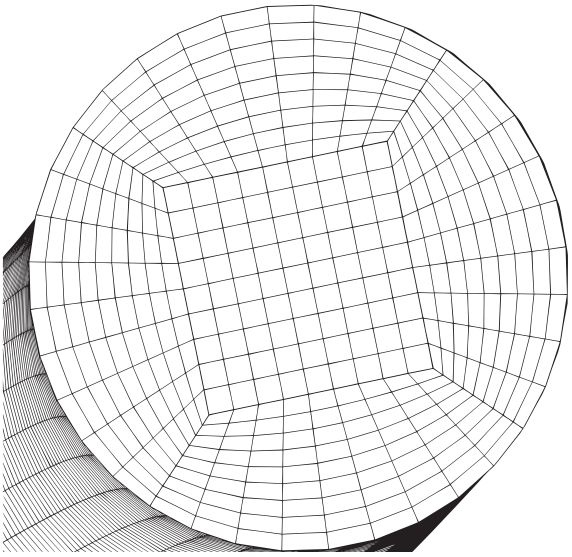

Fig. 5. Example of the mesh adopted for the numerical simulations.

The mean quadratic relative error of each of the adopted correlation is computed as:

$$\overline{e}_{\%} = \sqrt{\frac{1}{n}\sum_{i=1}^{n}\frac{\left(f_{m,i} - f_{c,i}\right)^2}{f_{m,i}^2}} \tag{6}$$

where f_m is the measured friction factor while f_c is the one predicted by the correlation. Results for the various correlations are reported in Table 3 for both laminar and transition regions. In the laminar region the lowest mean error is obtained with the Ito correlation. In the transition region ($3200 < Re < 5000$) rises in the computed error are quite limited and correlations that underestimated f_D at low flow rates agree better with experimental data due to the particular trend of the friction coefficient (i.e. the Barua and Srinivasan correlations). To sum up, we might state that the presented correlations work quite well also in the transition region,

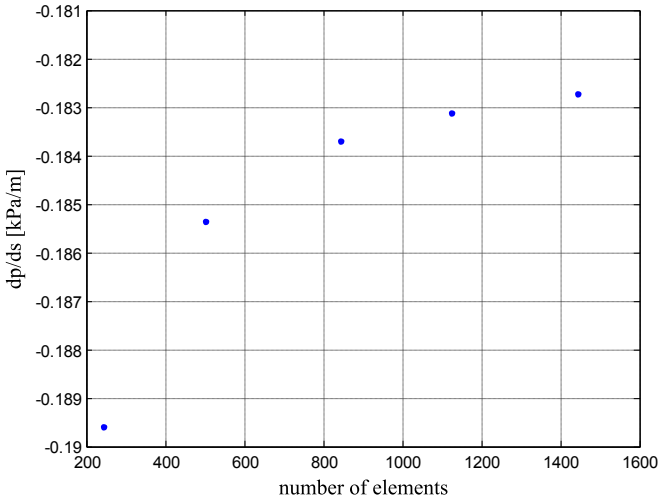

Fig. 6. Trend of the pressure gradient with number of nodes in the section mesh.

at least for geometries comparable to the one adopted in our measurements. Moreover, the Ito correlation is suggested for both the laminar and the transition regimes, since it returned the best results among all the correlations considered.

4. The numerical study

Different numerical codes are available in order to get an approximate solution of the hydrodynamic problem. Three of them have been tested in this work to verify their capability to reproduce the flow field and the friction pressure drop in helical tubes. For this reason their results have been compared with the experimental data and the correlations presented in the previous section. Computational Fluid Dynamics (CFD) simulations were made through the commercial software ANSYS FLUENT 14.0 (ANSYS FLUENT, 2011) and the open source code OpenFOAM. Both are based on the Finite Volume Method (FVM); in addition OpenFOAM is an open source instrument and thus has the advantage to be completely editable and controllable by the user. The Finite Element Method (FEM) based COMSOL Multiphysics (COMSOL, 2008) code was also used: this tool allows to simulate complex systems, in which different coupled phenomena occur at the same time. This approach is extremely useful for the research on innovative nuclear plants, which requires the parallel resolution of the thermal, neutronic, mechanical and chemical problems to fully characterize the dynamics of the system. As concerns the computations, the incompressible, laminar, steady Navier–Stokes equations were solved imposing a non-slip condition at the pipe wall, a constant pressure at the outlet and a velocity profile at the inlet. In particular such profile determines the length of the pipe at which

Table 4
Data of the sensitivity analysis performed with OpenFOAM®.

Coil 02		Coil 04		Coil 06		Coil 08		SIET	
Elements	dp/ds	Elements	dp/ds	Elements	dp/ds	Elements	dp/ds	Elements	dp/ds
245	−0.5605	245	−0.1896	245	−0.2467	320	−0.1259	1125	−0.01557
405	−0.5642	500	−0.1854	405	−0.2471	405	−0.1244	2000	−0.01557
605	−0.5588	845	−0.1837	605	−0.2467	500	−0.1257	2420	−0.01557
720	−0.5567	1125	−0.1831	1125	−0.2463	720	−0.1256	2880	−0.01558
		1445	−0.1827	2000	−0.2462	1125	−0.1255		
				3125	−0.2459				
				4500	−0.2457				

Table 5
Data of the helices used for the numerical simulations.

Helix	R	p_s	κ_{ad}	τ_{ad}	λ
H_1	0.1 m	0.02 m	0.09615	0.01923	0.2
H_2	0.1 m	0.05 m	0.08	0.04	0.5
H_3	0.1 m	0.1 m	0.05	0.05	1
H_4	0.1 m	0.2 m	0.02	0.04	2
H_5	0.1 m	0.5 m	0.00385	0.01923	5

fully developed flow is obtained: thus, in every case we verified that such conditions were reached before the end of the tube.

4.1. The mesh

A structured mesh was implemented by sweeping a planar grid along the axial direction of the pipe. Such grid is composed of five sections: the central area of the tube was meshed with a square grid, while the sides were constructed in a polar form, to obtain a

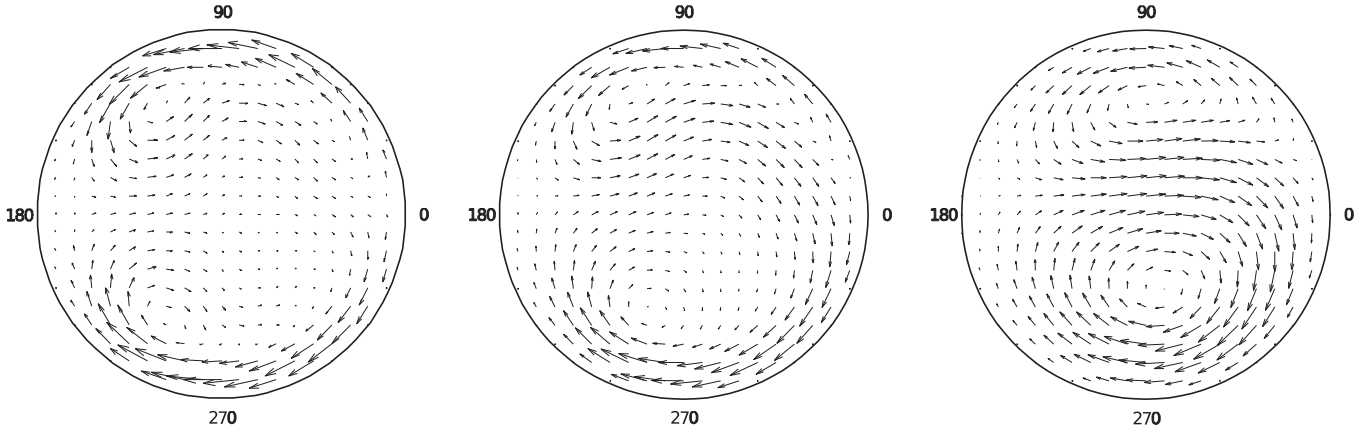

Fig. 7. Secondary velocity field within the cross sectional area of the tube at growing values of the torsion ratio λ and *Re* equal to 1000.

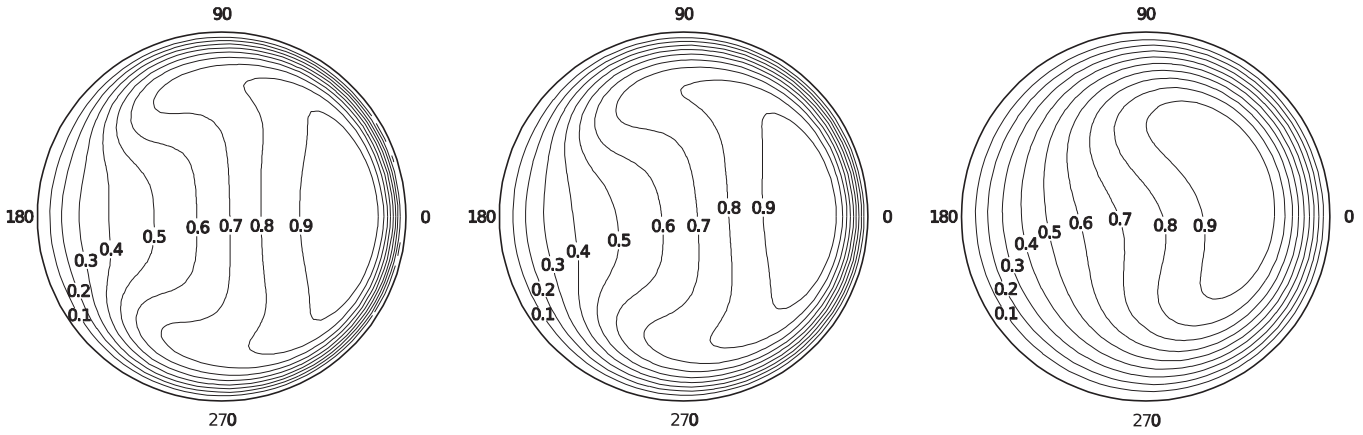

Fig. 8. Axial velocity field within the section with growing value of the torsion ratio λ and *Re* equal to 1000.

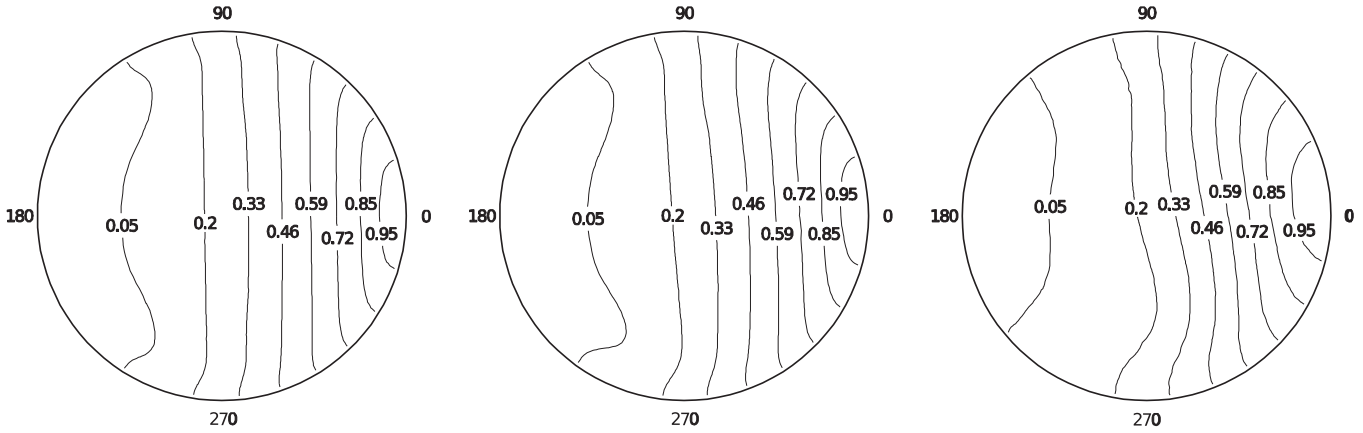

Fig. 9. Pressure field within the cross sectional area of the pipe at growing values of the torsion ratio λ and *Re* equal to 1000.

finer mesh near the wall while maintaining a proper spacing in the other regions, where such refinement was not necessary. The grid used for the simulations is presented in Fig. 5. A grid sensitivity study was performed, to define the optimal number of elements: different simulations of the same tube at the same conditions (fluid properties, inlet flow rate and outlet pressure) were performed with several meshes characterized by different node densities. As a result, a general converging trend of the results with respect to the number of nodes in the sectional grid was found: we chose the pressure gradient in the longitudinal direction as a term of comparison. Table 4 contains the results of such analysis with OpenFOAM and FLUENT (for which the same mesh for each case was adopted): in general the value of the pressure gradient converges to a stationary value, as can be seen in Fig. 6. We need to point that such a complete analysis was not performed with COMSOL Multiphysics because of the high computational times required by the solver. However, results were close to the ones obtained with the other packages as shown in the following sections.

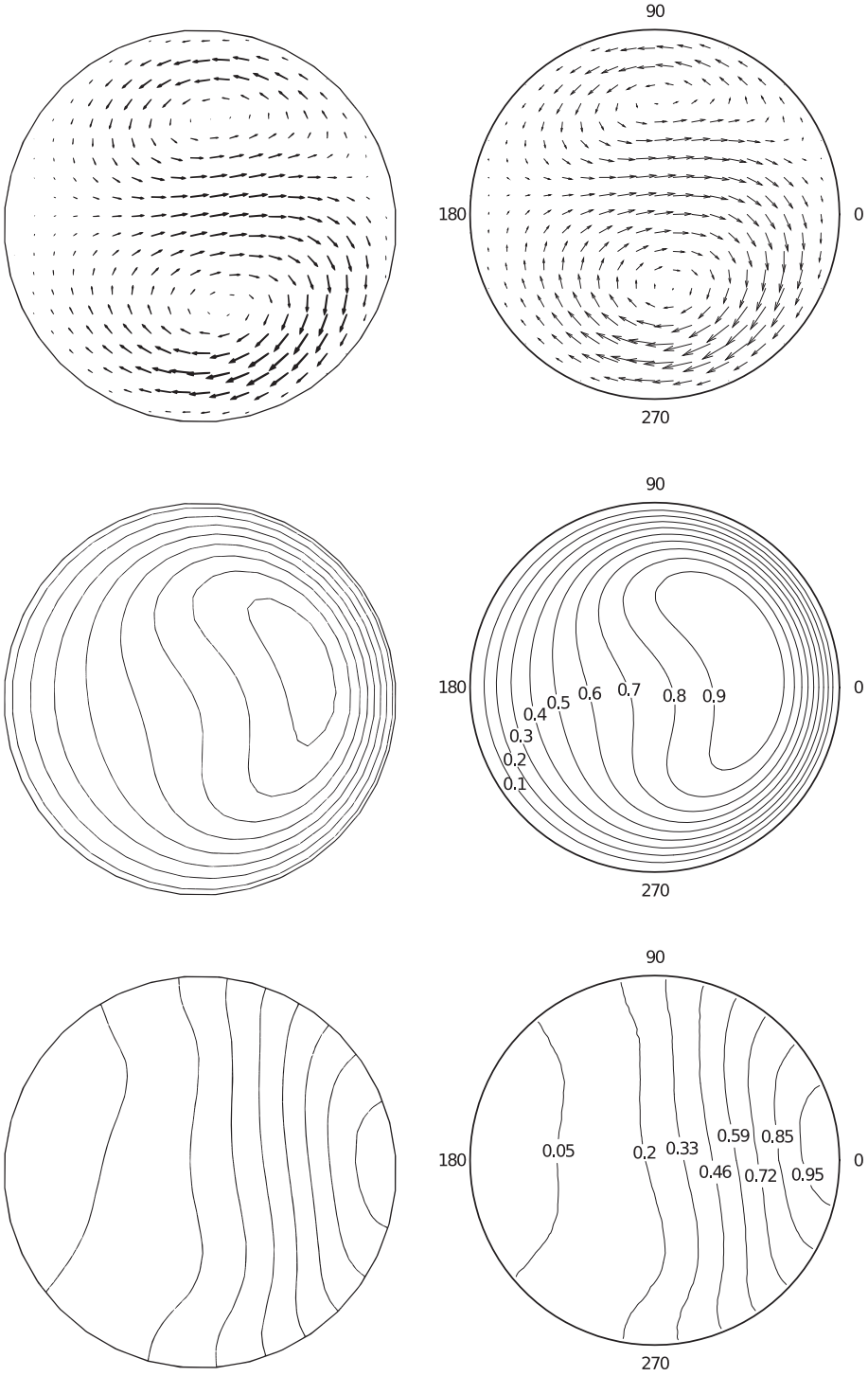

Fig. 10. Comparison between COMSOL (on the left) and FLUENT (on the right).

Table 6
Geometrical data of the helical coiled pipes used for comparison between experimental measurements, correlations ad computational results.

Helix	r	R	p_s	κ_{ad}	τ_{ad}	λ
SIET	6.265 mm	0.50 m	0.127 m	0.0118	3.00×10^{-3}	0.255
Coil 02	3.40 mm	0.057 m	2.87 mm	0.0593	2.97×10^{-3}	0.0501
Coil 04	5.22 mm	0.184 m	3.18 mm	0.0283	4.53×10^{-4}	0.0173
Coil 06	3.40 mm	0.184 m	3.18 mm	0.0188	3.29×10^{-4}	0.0175
Coil 08	4.30 mm	0.365 m	3.50 mm	0.0118	1.13×10^{-4}	0.00960

4.2. The effect of geometry

In order to evaluate the effect of geometrical parameters on the laminar flow, in particular on the emergence of secondary flows and on the breaking of the axial symmetry of the velocity field, a first set of five helices was simulated with COMSOL Multiphysics and FLUENT. Two packages were used also to compare their abilities to estimate the velocity and pressure fields within the domain. All the pipes present the same internal radius of 1 cm. The length of the pipes guarantees fully developed flow condition, necessary for a correct evaluation of the friction coefficient. In this set of simulations, the pitch per radiant p_s was varied at a fixed value of the coil radius R, to analyze the effect of the torsion parameter, defined as the ratio between dimensionless torsion and curvature ($\lambda = \tau_{ad}/\kappa_{ad} = p_s/R$). Geometrical parameters of the simulated coils are reported in Table 5.

Results show an increasing deformation of the structure of Dean's vortices with increasing torsion, which breaks the symmetry of the solution predicted by Dean (Dean, 1927, 1928). The two vortices, starting from an almost symmetrical configuration for $\lambda = 0.2$, change in dimensions, with the lower one enlarging while the upper one is pushed toward the upper wall, as shown in Fig. 7. The increase in torsion also produces a progressive deformation of the axial velocity field: its maximum value is displaced from the radial direction of the helix of an angle that is dependent on the value of the torsion parameter, as evident from Fig. 8. In addition, a distortion of the pressure field, that actually drives and sustains the secondary flow inside the section, is evident from the computations, in agreement with the results of other authors (Yamamoto et al., 1995). As shown in Fig. 9, constant pressure lines tend to become coarser toward the lower side of the tube and to concentrate at the opposite direction. This effect is connected to the formation of a low pressure region in the area near the center of the lower vortex, which appears clearly at higher values of the torsion ratio, such as λ ~10, as investigated in Hüttl et al. (1999). Both

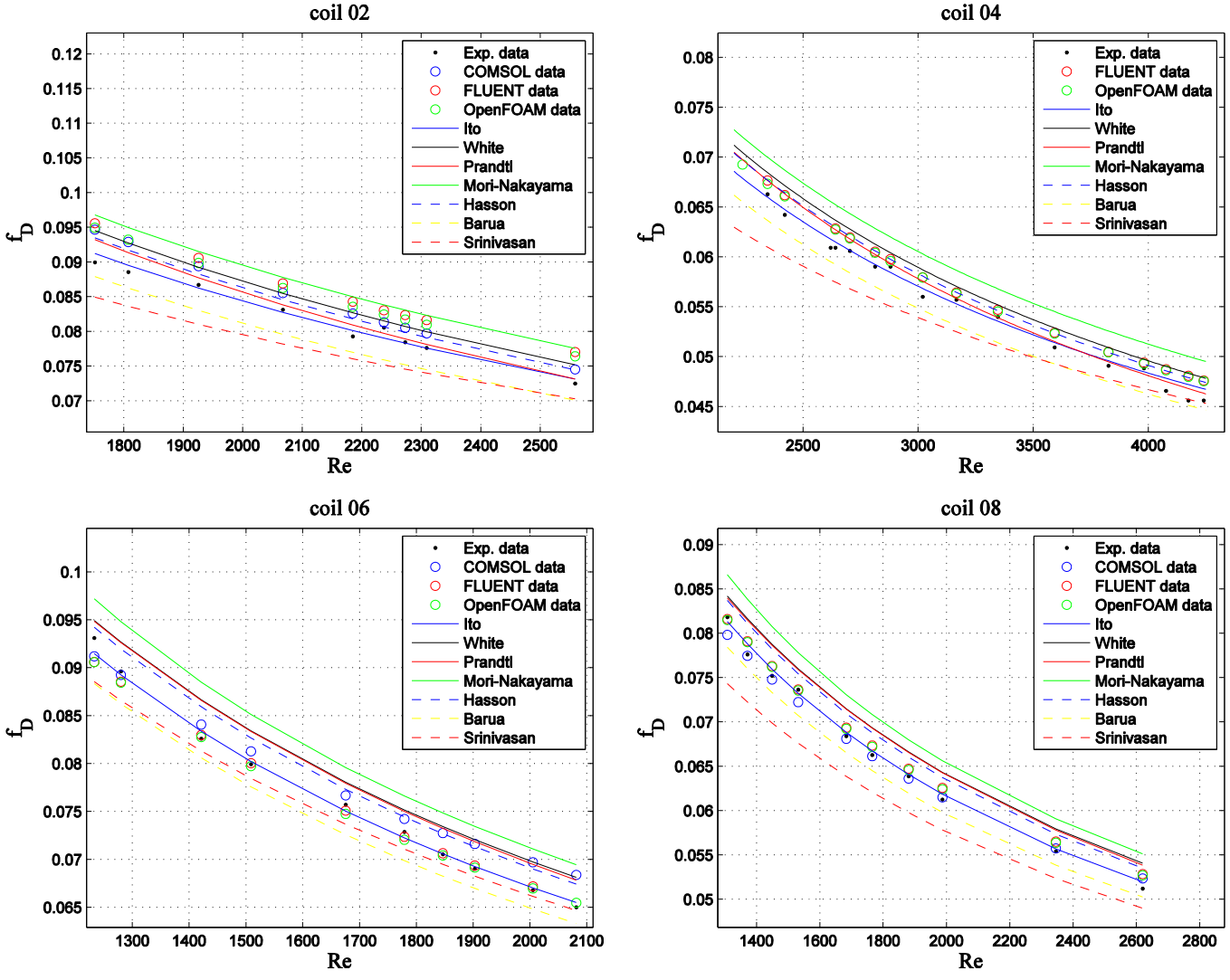

Fig. 11. Behavior of the Darcy friction factor f_D with Reynolds number for helical coils presented in Cioncolini and Santini (2006).

COMSOL and FLUENT are able to catch the main characteristics of the flow, as can be seen in Fig. 10. The slightly poorer quality of the profiles given by the FEM package is due to the lower grid density in the mesh, which was chosen as a consequence of the high computational times required by the software.

4.3. Validation of numerical codes

In order to validate the numerical results, a comparison with the experimental data of pressure losses was performed: in particular, the estimated friction factor was taken as a term of comparison. In addition to the measurements discussed previously, some other presented in Cioncolini and Santini (2006) were taken to extend the range of geometric parameters considered in the confrontation. All the numerical codes were adopted here so that a comparison of their capability to reproduce experimental data could be performed. The geometrical data of the simulated pipes are reported in Table 6: these are the SIET pipe and coils 02, 04, 06 and 08 from Cioncolini and Santini (2006). In particular, coil 02 has a strong curvature, characterized by a unique discontinuity in the behavior of the friction factor as a function of the Reynolds number, while the other coils have a medium curvature, thus presenting a slight depression in the profile of f_D between the fully laminar and turbulent regimes. According to the classification of Cioncolini, the coil installed at SIET belongs to the latter group. In order to obtain the friction factor, the difference between the average pressure at two sections of the pipe, positioned far from outlet and inlet boundaries, was calculated and substituted in Eq. (5). Numerical results show a fair agreement with empirical correlations and experimental friction factors presented in Cioncolini and Santini (2006), which are shown in Fig. 11. As concerns the SIET duct, results of the computations are compared with experimental data in Fig. 12: numerical results are in good agreement with the experimental data and the literature correlations. Being the numerical models based on laminar flow, a certain divergence between the numerical results and the experimental values of f_D is detectable for Re ~3200, where the turbulence onset appears.

As regards the comparison between the different numerical codes used in the computations, all of them are in good agreement with the experimental measurements and the empirical correlations. The maximum error between the measured and the computed values of f_D is about 5% for all the numerical codes taken in consideration. In Table 7 the quadratic mean errors of the friction factor computed by the different packages for the considered geometries with respect to the experimental values are presented. It is interesting to note that, despite a coarser mesh, errors obtained with COMSOL are of the same order of magnitude of those obtained with FLUENT and OpenFOAM. Instead marked differences in the computational times required by FVM and FEM software were found: in particular, the latter needed a larger time for reaching convergence, especially for high values of the inlet flow rate. A detailed study of the causes of this problem was beyond the objective of this work. Conversely, from a more practical point of view, the post-processing tools offered by the commercial packages, especially by COMSOL, allow a complete and steady analysis of the results of the computations, without creating external scripts to obtain quantitative information from the simulations, as required for OpenFOAM. This is due to the helical geometry that does not allow an immediate definition of the cut planes necessary to display correctly the velocity and pressure fields within a cross section.

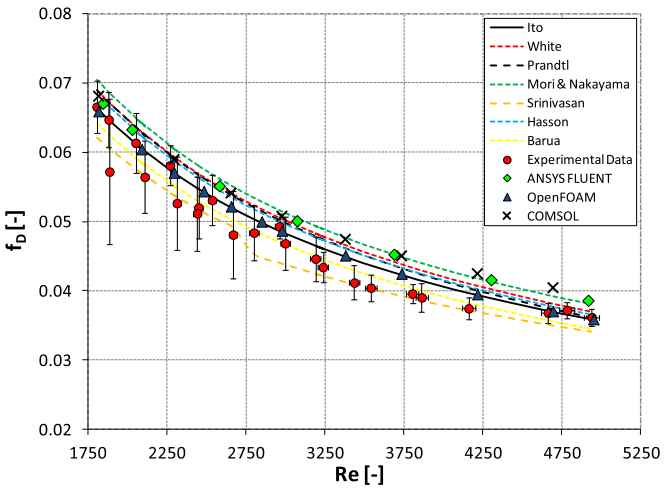

Fig. 12. Behavior of the Darcy friction coefficient with Reynolds number for SIET helix.

Table 7
Root mean square errors of computed friction factors from experimental ones for the performed simulations.

	COMSOL	FLUENT	OpenFOAM
Coil 02	3.36%	4.68%	4.33%
Coil 04	–	2.95%	2.72%
Coil 06	2.74%	1.17%	1.27%
Coil 08	1.24%	1.68%	1.51%
Coil SIET	4.29%	–	2.56%

5. Conclusions

An analysis of the steady incompressible adiabatic laminar flow in helically coiled pipes was carried out in order to better understand the effect of the helical geometry on the flow field. In particular, a new experimental campaign was performed to collect pressure drop experimental data in a helical tube of the SG of an innovative SMRs. Pressure losses were measured in laminar, transition and turbulent regimes, in order to further evaluate and compare different empirical correlations for the determination of the friction factor. The laminar to turbulent transition was well predicted with the correlation proposed in Cioncolini and Santini (2006), which describes the trend of the critical Reynolds number as a function of the geometrical parameters of the tube. As concerns the friction coefficient, Ito's correlation returned the lowest mean errors. In addition, almost all the correlations showed a very limited increase in their uncertainties in the evaluation of the friction factor also in the transition region (up to Re ~ 5000 for the studied helix). A numerical analysis was made in order to verify the capability of the different numerical codes to predict different quantities of interest in helically coiled pipes, in particular the friction coefficient. Three numerical codes were tested, the ANSYS FLUENT and OpenFOAM FVM codes and the COMSOL Multiphysics FEM package. We found that results were in agreement with previous analyses conducted by other authors in the past and between the different adopted tools. Numerical values of the Darcy friction factor were compared to several empirical correlations and different experimental data, from both the new measurements and a previous literature work, showing maximum deviations of the order of few percent.

Acronyms

CFD	computational fluid dynamics
DWO	density wave oscillation
FEM	finite element method

FVM	finite volume method
GIF	Generation IV International Forum
IRIS	International Reactor Innovative and Secure
NPP	nuclear power plant
SG	steam generator
SMART	System integrated Modular Advanced ReacTor
SMR	Small-medium Modular Reactor

Nomenclature

De	Dean Number [−]
d	tube diameter [m]
f	friction factor of the coiled tube [−]
L	tube length [m]
p	pressure [Pa]
p_s	helix pitch per radiant [m/rad]
R	helix radius [m]
Re	Reynolds number [−]
r	tube radius [m]
s	axial coordinate [m]
T	temperature [°C]
u	average axial velocity [m/s]
u_{max}	maximum of the axial velocity [m/s]

Greek symbols

β	helix angle of inclination [−]
$\beta_0 = \tau_{ad}/(2\ \kappa_{ad})^{0.5}$	torsion parameter [−]
$\kappa = R/(R^2 + p_s^2)$	helix curvature [m^{-1}]
$\kappa_{ad} = rR/(R^2 + p_s^2)$	helix non-dimensional curvature [−]
$\lambda = \tau_{ad}/\kappa_{ad}$	torsion ratio [−]
ρ	fluid density [kg m^{-3}]
$\tau = p_s/(R^2 + p_s^2)$	helix torsion [m^{-1}]
$\tau_{ad} = rp_s/(R^2 + p_s^2)$	helix non-dimensional torsion [−]

Subscripts

c	coiled tube
crit	critical
D	Darcy
s	straight tube

References

Ali, S., 2001. Pressure drop correlations for flow through regular helical coil tubes. Fluid. Dyn. Res. 28 (4), 295–310.

ANSYS FLUENT 14.0 User Guide, 2011.

Barua, S.N., 1963. On secondary flow in stationary curved pipesm. Q. J. Mech. Appl. Math. 16, 61–77.

Bejan, A., Kraus, A.D., 2003. Heat Transfer Handbook. Wiley.

Berger, S.A., Talbot, L., Yao, S.L., 1983. Flow in curved pipes. Annu. Rev. Fluid Mech. 15, 461–512.

Carelli, M.D., Conway, L.E., Oriani, L., Petrovic, B., Lombardi, C.V., Ricotti, M.E., Barroso, A.C.O., Collado, J.M., Cinotti, L., Todreas, N.E., Grgic, D., Moraes, M.M., Boroughs, R.D., Ninokata, H., Ingersoll, D.T., Oriolo, F., 2004. The design and safety features of the IRIS reactor. Nucl. Eng. Des. 230 (1), 151–167.

Cioncolini, A., Santini, L., 2006. An experimental investigation regarding the laminar to turbulent flow transition in helically coiled pipes. Exp. Therm. Fluid Sci. 30, 367–380.

COMSOL, Inc., 2008. COMSOL Multiphysics® User's Guide, Version 3.5a.

Dean, W.R., 1927. Note on the motion of fluid in a curved pipe. Philos. Magn. 4, 208–223.

Dean, W.R., 1928. The stream-line motion of fluid in a curved pipe. Philos. Magn. 5, 673–695.

Eustice, J., 1910. Flow of water in curved pipes. Proc. Roy. Soc. A Math. Phys. 84, 107–118.

Generation IV International Forum, GIF Annual Report 2010.

Germano, M., 1982. On the effect of torsion on a helical pipe flow. J. Fluid Mech. 125, 1–8.

Germano, M., 1989. The Dean equations extended to a helical pipe flow. J. Fluid Mech. 203, 289–305.

Greenspan, D., 1973. Secondary flow in a curved pipe. J. Fluid Mech. 57, 167–176.

Hasson, D., 1955. Streamline flow resistance in coils. Res. Corresp. 1, S1.

Hüttl, T.J., Wagner, C., Friedrich, R., 1999. Navier-Stokes solutions of laminar flows based on orthogonal helical co-ordinates. Int. J. Numer. Methods Fluids 29, 749–763.

IAEA, 2005. Innovative Small and Medium Sized Reactors: Design Features, Safety Approaches and R&D Trends. IAEA-TECDOC-1451.

Ito, H., 1959. Friction factors for turbulent flow in curved pipes. J. Basic Eng. Trans. ASME 81, 123–124.

Ito, H., 1969. Laminar flow in curved pipes. Zamm-Z. Angew. Math. Met. 49, 653–663.

Kim, S.H., Kim, K.K., Yeo, J.W., Chang, M.H., Zee, S.Q., 2003. Design verification program of SMART. In: International Conference on Global Environment and Advanced Nuclear Power Plants, Kyoto, Japan, 15–19 September.

McConalogue, D.J., Srivastava, R.S., 1968. Motion of a fluid in a curved tube. Proc. Roy. Soc. A Math. Phys. 307, 37–53.

Mori, Y., Nakayama, W., 1965. Study on forced convective heat transfer in curved pipes. Int. J. Heat Mass Trans. 8, 67–82.

Murata, S., Miyake, Y., Inaba, T., Ogawa, H., 1981. Laminar flow in a helically coiled pipe. Bull. JSME 24, 335–356.

Naphon, P., Wongwises, S., 2006. A review of flow and heat transfer characteristics in curved tubes. Renew. Sust. Energ. Rev. 10, 463–490.

Papini, D., Cammi, A., Colombo, M., Ricotti, M.E., 2011. On density wave instability phenomena: modelling and experimental investigation. In: Ashan, A. (Ed.), Two-phase Flow, Phase Change and Numerical Modelling. InTech Publisher, Rijeka, pp. 257–284.

Papini, D., Colombo, M., Cammi, A., Ricotti, M.E., 2014. Experimental and theoretical studies on density wave instabilities in helically coiled tubes. Int. J. Heat Mass Trans. 68, 343–356.

Prandtl, L., 1949. Fuhrer dmchdie stromungslehre (Essentials of Fluid Dynamics). Braunsschweigh, third ed. Blackie and Son, London. 1954.

Santini, L., Cioncolini, A., Lombardi, C., Ricotti, M., 2008. Two-phase pressure drops in a helically coiled steam generator. Int. J. Heat Mass Trans. 51, 4926–4939.

Srinivasan, P.S., Nandapurkar, S.S., Holland, F.A., 1968. Pressure drop and heat transfer in coils. Chem. Eng. J. 218, 113–119.

Wang, C.Y., 1981. On the low-Reynolds number flow in a helical pipe. J. Fluid Mech. 108, 185–194.

White, C.M., 1929. Streamline flow through curved pipes. Proc. Roy. Soc. A Math. Phys. 123, 645–663.

Yamamoto, K., Akita, T., Ikeuchi, H., Kita, Y., 1995. Experimental study of the flow in a helical circular tube. Fluid. Dyn. Res. 16, 237–249.